

Letter

Comparison of Hyperspectral Versus Traditional Field Measurements of Fractional Ground Cover in the Australian Arid Zone

Claire Fisk , Kenneth D. Clarke and Megan M. Lewis

School of Biological Sciences, The University of Adelaide, Adelaide 5005, Australia; kenneth.clarke@adelaide.edu.au (K.D.C.); megan.lewis@adelaide.edu.au (M.M.L.)

* Correspondence: claire.fisk@adelaide.edu.au

Received: 1 October 2019; Accepted: 26 November 2019; Published: 28 November 2019



Abstract: The collection of high-quality field measurements of ground cover is critical for calibration and validation of fractional ground cover maps derived from satellite imagery. Field-based hyperspectral ground cover sampling is a potential alternative to traditional in situ techniques. This study aimed to develop an effective sampling design for spectral ground cover surveys in order to estimate fractional ground cover in the Australian arid zone. To meet this aim, we addressed two key objectives: (1) Determining how spectral surveys and traditional step-point sampling compare when conducted at the same spatial scale and (2) comparing these two methods to current Australian satellite-derived fractional cover products. Across seven arid, sparsely vegetated survey sites, six 500-m transects were established. Ground cover reflectance was recorded taking continuous hyperspectral readings along each transect while step-point surveys were conducted along the same transects. Both measures of ground cover were converted into proportions of photosynthetic vegetation, non-photosynthetic vegetation, and bare soil for each site. Comparisons were made of the proportions of photosynthetic vegetation, non-photosynthetic vegetation, and bare soil derived from both in situ methods as well as MODIS and Landsat fractional cover products. We found strong correlations between fractional cover derived from hyperspectral and step-point sampling conducted at the same spatial scale at our survey sites. Comparison of the in situ measurements and image-derived fractional cover products showed that overall, the Landsat product was strongly related to both in situ methods for non-photosynthetic vegetation and bare soil whereas the MODIS product was strongly correlated with both in situ methods for photosynthetic vegetation. This study demonstrates the potential of the spectral transect method, both in its ability to produce results comparable to the traditional transect measures, but also in its improved objectivity and relative logistic ease. Future efforts should be made to include spectral ground cover sampling as part of Australia's plan to produce calibration and validation datasets for remotely sensed products.

Keywords: calibration; ground cover; hyperspectral; spectral unmixing; validation

1. Introduction

Satellite image-derived fractional ground cover mapping has proven to be an essential source of information for applications, including analysis of spatial and temporal vegetation dynamics [1], monitoring urban greenness [2], mapping bushfire burn severity levels [3], forest cover change [4], and deforestation [5]. Algorithms, including spectral mixture analysis [6–8], multiple endmember spectral mixture analysis [9], and relative spectral mixture analysis [10], are used to produce fractional cover (FC) maps. These algorithms can be applied to multispectral and hyperspectral imagery, decomposing each image pixel into a measure of similarity to two or more spectrally distinct land cover types. These

typically include photosynthetic vegetation (PV), non-photosynthetic vegetation (NPV), bare soil (BS), shadow, and snow [6,10], with the resulting maps providing quantitative estimates of the proportion of the cover types comprising each pixel.

Fractional cover mapping has been performed across a range of scales, including global mapping projects as such the Copernicus Global Land Service, which has produced a 300-m and a 1-km fraction of green vegetation cover product based on PROBA-V and SPOT-VGT imagery [11,12]. Local studies have used FC products to assist water quality management of catchments [13], urban land cover mapping [14], and the study of savanna vegetation morphology [15,16]. In Australia, time series of fractional cover have been produced from MODIS [17] and Landsat [18,19] and are being used widely for environmental assessment and monitoring applications.

Calibration and validation are essential for ensuring the reliability and consistency of FC products. Data used for calibration and validation of fractional cover are derived from a variety of sources and techniques, and there is currently no international standard. Lawley et al. [20], Montesano et al. [21], Morissette et al. [22], and Xiao and Moody [23] all utilised remotely sensed imagery with high spatial resolution to validate FC products with lower spatial resolution. The advantages of this approach are that high-spatial resolution imagery provides an objective record at the time of the region being assessed and may allow for the validation of areas that cannot be easily accessed. Alternative evaluations have sought to avoid subjective on-ground assessments of ground cover and instead have used a combination of qualitative and quantitative data for assessment. For example, Guerschman et al. [16] utilised two qualitative datasets to calibrate the Australian MODIS fractional cover product: (1) A general description of vegetation type and condition, including photographs of each site, and (2) a vectorized fire scar map that classified areas of the landscape as either burnt or unburnt.

Common approaches to in situ measurement of ground cover, demonstrated by Scarth, Röder, and Denham [24], Asner and Heidebrecht [25], and Lewis [26], have utilised variants of point-based sampling techniques that were initially developed for vegetation ecology and rangeland assessment [27–29]. These methods include line-point intercept transects, step-point surveys, and wheel-point surveys, where observers walk across a study area making point-based observations at defined intervals. Across a survey area, hundreds of point-based observations are used to estimate FC. Point observations generally categorise ground cover into defined classes, such as rock, disturbed soil, green leaf, and dry leaf, which are later aggregated into broader classes, such as PV, NPV, and BS, matching the field classes with the image product being assessed. Muir et al. [30] developed an Australian national standard for field measurements of fractional ground cover, which provides a well-documented, easily repeatable method that is now widely used.

Although field protocols have been developed to improve consistency and reduce the potential for errors, subjective human judgements are still required, and these may affect the data significantly [31]. In such surveys, observers are required to make hundreds of rapid decisions, only having a few seconds to observe and record the cover type before moving on. Most cover types are relatively easy to discriminate in the field but distinguishing between PV and NPV can be a difficult task. PV and NPV are better thought of as extremes of a continuum, rather than binary categories, and hence distinguishing between PV and NPV can be difficult for observers [32].

A technique that has the potential to help reduce subjectivity is to estimate the relative fractions of PV, NPV, and BS from field-based hyperspectral reflectance measurements. While in situ hyperspectral measurements have been used for radiometric and spectral calibration and validation of remotely sensed products [33,34], and may provide reference signatures for image analyses [17,18], they have not been used explicitly for the validation of fractional ground cover products until Meyer and Okin [35]. This method records many in situ spectra over a study area, which in their aggregate, capture the combined spectral response of the site. The relative proportions of PV, NPV, and BS can then be unmixed from the field spectra. Using this approach Meyer and Okin [35] demonstrated a stronger agreement between FC values derived from field-based reflectance measurements and their image-based product than between traditional line-point intercept observations and their image-based product, which

showed low correlations. In our paper, hyperspectral ground surveys refer to the collection of spectral measurements over an area for the purpose of estimating ground cover fractions [33], quite a different application to the use of in situ spectroscopic measurements for radiometric calibration of imagery.

Another challenge for calibration and validation is to match the scale of field data with that of broad-scale FC products. When validating products developed from coarse resolution imagery (e.g., 500 m), it is common to up-scale field data recorded at a finer scale (e.g., 100 m) in order to determine the accuracy of the coarse resolution products. This is usually conducted under the assumption that the area around the sample site is homogenous and similar to that surveyed. For example, Meyer and Okin [35] conducted spectral sampling over 500-m transects to correspond to a MODIS pixel and compared the results to line-point intercept sampling that was conducted over smaller 100-m transects. A potential reason for the low correlation between the sampling methods is that the 100-m transects were insufficient to gain an adequate estimate of the ground cover for a 500-m pixel. Meyer and Okin [35] were following the Muir et al. [30] field sampling layout, where transects were placed in a radiating star pattern that was designed to relate field measurements to Landsat imagery. The Muir et al. [30] design samples three 100-m transects, which covers approximately 3×3 Landsat pixels, making it ideal for validating Landsat-based products but not necessarily adequate for coarser resolution products (MODIS).

The layout of transects also has the potential to affect how an area is sampled. For instance, the star-transect method includes a sampling bias that over-represents cover towards the centre of the plot. Three transects are placed in a star pattern with the result being that observation points are concentrated in the centre of the star and increasingly dispersed as the distance from the centre increases. Therefore, a sampling pattern that provides a more even distribution across a site may provide a better representation of the ground cover. Other studies have placed parallel transects evenly across sample sites [26,36] or placed transects in a grid pattern in order to more evenly sample the area [37].

Field-based hyperspectral ground cover sampling is a potential alternative to traditional techniques that may assist with the calibration and validation of remotely sensed products. The motivation for this research is to expand upon the work of Meyer and Okin [35] and trial hyperspectral ground cover sampling in Australia, with the ultimate aim of incorporating spectral sampling as part of Australia's national effort to collect validation and calibration data to meet our remote sensing needs. Our aim was to develop an effective sampling design for spectral ground cover surveys in order to estimate fractional ground cover. Our objectives were (1) to determine how spectral surveys and traditional step-point sampling compare when conducted at the same spatial scale, and (2) determine how these in situ methods compare to current Australian satellite-derived FC products.

2. Materials and Methods

Currently, in situ validation data collected using the Muir et al. [30] method is used to assess the accuracy of both the MODIS and Landsat products. Meyer and Okin [35] found that the in situ spectral measurements they collected could be used to validate fractional ground cover mapping developed from MODIS imagery over Botswana, but this has not been tested across other environments. To meet our objectives, we therefore completed ground cover surveys before inspecting how our in situ measurements would compare with the MODIS and Landsat products. Figure 1 provides an overview of the methods used in this study.

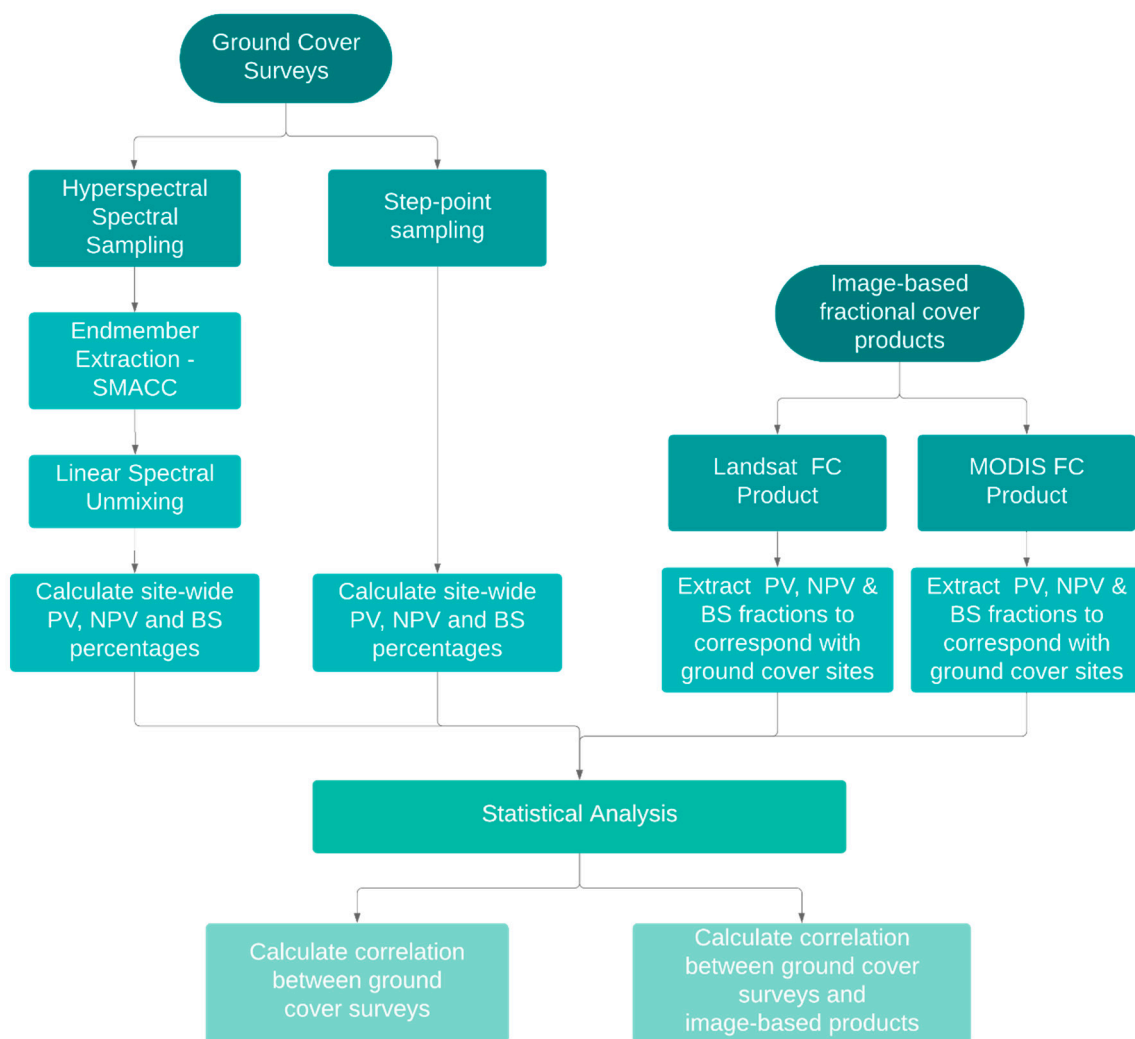


Figure 1. Flowchart outlining the methodological approach taken in this paper.

2.1. Study Area

The study was conducted in New South Wales (NSW), Australia within the arid zone (Figure 2). Sites FG1–FG4 (Figure 3a,b) were situated at Fowlers Gap Arid Research Station, 110 km north of Broken Hill, NSW, while sites BH1–BH3 (Figure 3c,d) were located surrounding the City of Broken Hill. The climate for both regions is hot and persistently dry [38]. Fowlers Gap has a mean annual rainfall of 240 mm, a mean annual minimum temperature of 13 °C, and a mean annual maximum temperature of 26.9 °C [39]. The vegetation at Fowlers Gap comprises low open chenopodiaceous shrublands, some low open *Acacia* and *Casuarina* woodland as well as grasslands on the plains Mabbutt et al. [40]. Broken Hill has a mean annual rainfall of 250 mm with a mean annual minimum temperature of 11.8 °C and a mean annual maximum temperature of 24.7 °C [41]. The vegetation around Broken Hill is also composed of chenopod shrublands that includes saltbush and bluebush communities as well as Mulga (*Acacia aneura*) [42].

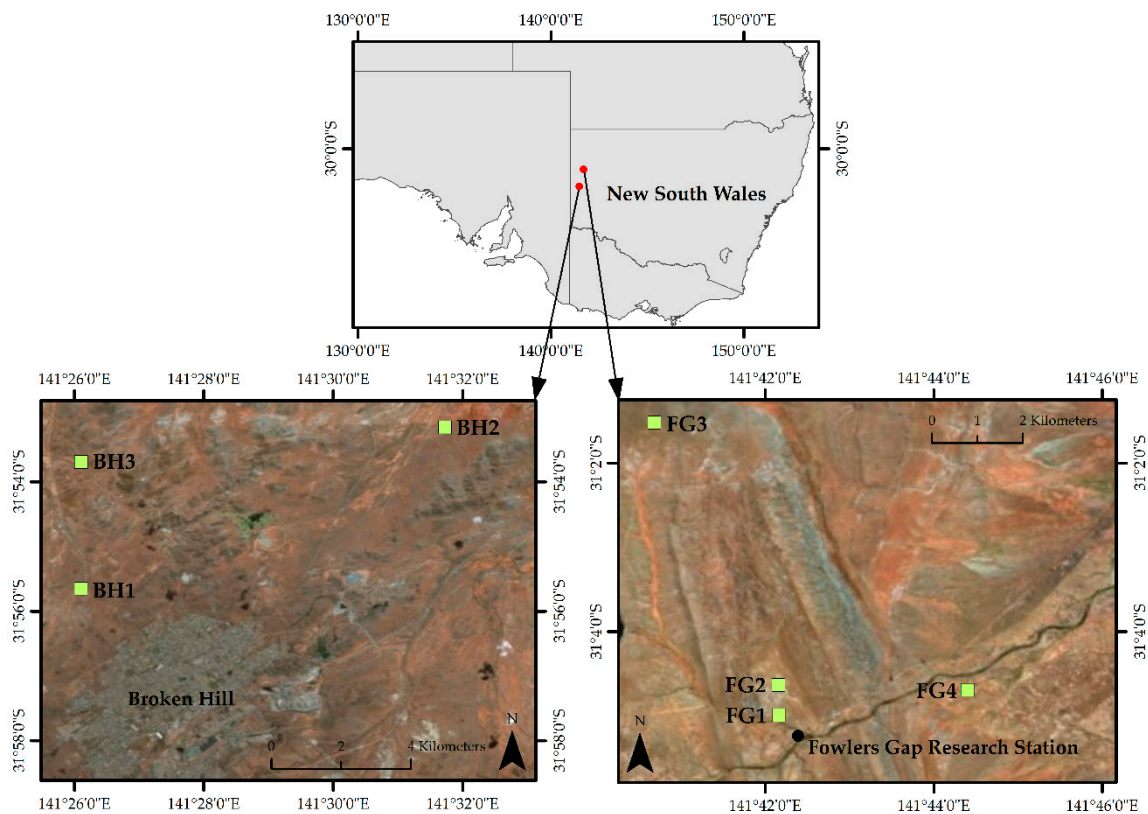


Figure 2. Site map displaying the locations of survey sites surrounding Broken Hill and Fowlers Gap Research Station, NSW. Base map: true colour satellite image accessed from ESRI, 2019.

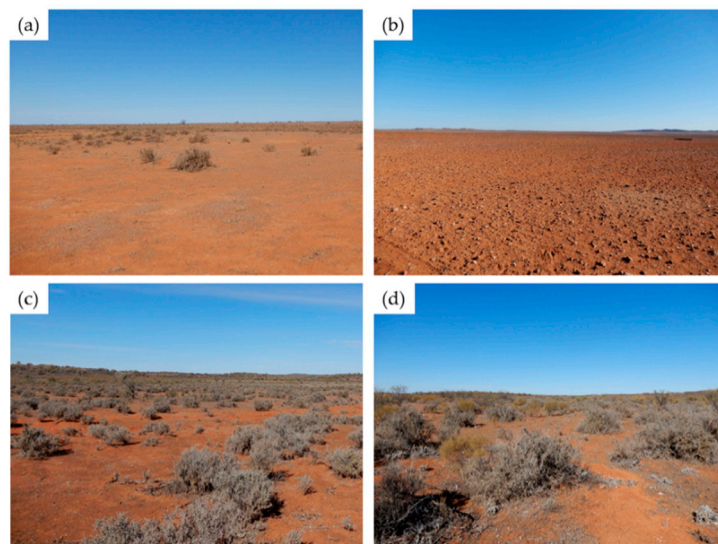


Figure 3. Site photographs from Fowlers Gap Research Station (a,b) and Broken Hill (c,d).

2.2. Ground Cover Surveys

To survey ground cover, six 500-m transects oriented north–south and spaced 100 m apart were established at each site. Across the six transects, two survey methods were used. Firstly, ground cover reflectance was recorded using an Analytical Spectral Devices Inc. FieldSpec 3 spectroradiometer (ASD) that measures the visible to shortwave infrared (350–2500 nm) parts of the electromagnetic spectrum. The sensor has 2150 bands with a spectral resolution of 3 nm from 350–1000 nm and 10 nm from 1000–2500 nm. An 8-degree field of view fore-optic was held 1 m above the ground, creating

a 0.14-m diameter ground field of view. At the start of each transect, and as required, the device was optimized and white reference measurements taken following the recommended protocols [43]. The operator of the ASD walked along each transect at a consistent pace taking continuous readings of ground cover reflectance. The continuous readings were averaged by the ASD and 10 averaged spectra were recorded for each 25-m segment of the transect, totalling 200 spectra per transect (1200 measurements per site).

The second method used was step-point sampling, where an observer collected point-based observations of ground cover along the six transects. The observer marked a point on a boot tip and at 5-m intervals recorded the cover that intersected the point. Cover was categorised into a set number of cover types, including crust, rock, litter, green leaf, and dry leaf, as outlined in the Muir et al. [30] protocol. The cover for each of these categories was calculated as the proportion of the total number of point observations at the site ($n = 600$). These categories were grouped into three broad classes, PV, NPV, and BS, to give their FC percentage within the site.

2.3. Endmember Extraction and Spectral Unmixing

The hyperspectral reflectance measurements for each transect were converted into single raster files enabling them to be processed in ENVI 5.3.1 (Exelis Visual Information Solutions, Boulder, Colorado). The Sequential Maximum Angle Convex Cone (SMACC) tool was used to extract endmembers from the transect rasters and to perform linear spectral unmixing [44]. The SMACC tool automatically defines the most extreme point (i.e., the brightest pixel in multi-dimensional space) as the first endmember in the raster using a convex cone model. The next endmember is identified based on the angle it makes with the existing cone (i.e., the pixel that is most different from the brightest), which is then added to the cone to derive the next endmember. This process continues until a specific tolerance is reached or until a specific number of endmembers are identified.

For each of the transects, PV, NPV, and BS endmembers (Figure 4) were extracted and abundance images of PV, NPV, BS, and shadow were produced, with each image displaying the proportion a specific endmember contributes to each pixel. These images were produced using a fully constrained linear spectral unmixing algorithm:

$$DN_b = \sum_{i=1}^n F_i DN_{i,b} + E_b \text{ and } \sum_{i=1}^n F_i = 1, \quad (1)$$

where DN_b is the apparent surface reflectance of a pixel in band b of an image; F_i is the fraction of endmember i ; $DN_{i,b}$ is the relative reflectance of endmember i in band b ; n is the number of endmembers; and E_b is the error for band b of the fit of n spectral endmembers, that of [7,8,45].

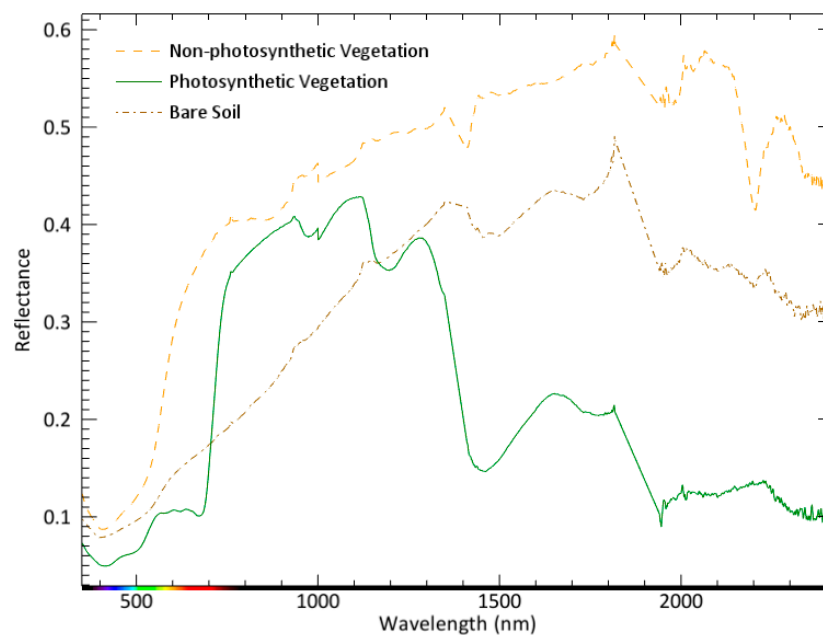


Figure 4. Example of image-derived endmembers for non-photosynthetic vegetation, photosynthetic vegetation, and bare soil.

The proportions of PV, NPV, and BS across each site were calculated as the averages of the unmixed fractions derived from each transect spectrum.

2.4. Comparison to Image-Based Fractional Cover Products

The field-based FC estimates were compared to two Australian image-derived FC products based on MODIS [46] and Landsat imagery [47]. The MODIS FC product was initially developed for monitoring the tropical savanna region of the Northern Territory, Australia [16] and was later applied across the continent by the Commonwealth Scientific and Industrial Research Organisation (CSIRO) [19]. This product uses MODIS imagery and describes the proportion of PV, NPV, and BS Australia-wide. The Landsat product was developed by the Joint Remote Sensing Research Program (JRSRP) also as a national FC product utilising the Landsat archive. Initially developed for rangeland monitoring in Queensland, Australia, the product is now being implemented nationally by Geoscience Australia [21,24]. Key differences between the two products include their spatial and temporal resolutions. The MODIS product has a moderate resolution of 500 m while the Landsat product is at a finer scale of 25 m. The latest version of the MODIS product uses MODIS MC43A4 version 6 imagery, which is a 16-day composition of daily captures from 2000 to 2019 (on-going) [46]. The Landsat product utilises data from the Landsat archive from 1986 to the present. Recent versions of the Landsat and MODIS FC products use a similar unmixing process [23] that incorporates endmembers of PV, NPV, and BS derived from field spectra and the imagery itself. For this study, the Guerschman and Hill [46] version 3.1.0 MODIS product and the Landsat FC25 version 1.5 were used [47]. The MODIS and Landsat FC products were acquired for dates that corresponded with the collection of in situ ground cover measurements. The Landsat FC image is based on a single date (17 August 2018) while the MODIS FC product is developed from a 16-day composite of imagery collected from the 13 to 28 August 2018. The PV, NPV, and BS values for each of the seven sites were extracted from a single pixel for the MODIS product while an average of 400 Landsat pixels across the same 500 × 500 m area were calculated. These extracted values were then compared to both the step-point and the spectral PV, NPV, and BS fractions.

2.5. Statistical Analysis

To determine the relationship between the in situ FC estimates and the image-based estimates, two metrics were used: Spearman's rank-order correlation (r_s) to measure the relationship between methods and the mean absolute error (MAE) to measure the average error. MAE was calculated as follows:

$$MAE = \frac{1}{n} \sum_{i=1}^n |f_1 - f_2| \quad (2)$$

where f_1 and f_2 represent the two FC measures being tested and n is the number of measurements. MAE is an average of the absolute difference between FC measure 1 and FC measure 2 (i.e., the absolute error). MAE is calculated in the same units as the variables and is a negatively oriented score, with lower values indicating lower errors.

3. Results

The in situ methods showed strong positive relationships across all three ground cover types (Table 1). While r_s was high, the MAE for NPV ($r_s = 0.61$, MAE = 19.82) and BS ($r_s = 0.82$, MAE = 19.26) was also relatively high. PV ($r_s = 0.87$, MAE = 1.37) showed a high correlation with low errors. Overall, low errors were observed for all comparisons made for PV. When the in situ methods were compared to the image-based models (MODIS and Landsat), spectral transect sampling showed a strong relationship to the MODIS image for PV and was the strongest relationship observed ($r_s = 0.91$, MAE = 4.21). For BS, the correlation between the MODIS imagery and the in situ methods was moderate and moderate to low for NPV. In comparison, the Landsat imagery showed a strong to moderate relationship with both in situ methods for BS, NPV, and PV.

Table 1. Summary of correlations and errors for each ground cover type based on comparisons between in situ and image-based fractional cover methods (step-point, spectral, MODIS, and Landsat).

Bare Soil				
	Step-point		Spectral	
	r_s	MAE	r_s	MAE
Step-point				
Spectral	0.82	19.26		
MODIS	0.58	20.31	0.56	26.43
Landsat	0.79	13.85	0.79	19.95
Non-photosynthetic Vegetation				
	Step-point		Spectral	
	r_s	MAE	r_s	MAE
Step-point				
Spectral	0.61	19.82		
MODIS	0.43	19.62	0.16	19.61
Landsat	0.68	15.79	0.71	14.86
Photosynthetic Vegetation				
	Step-point		Spectral	
	r_s	MAE	r_s	MAE
Step-point				
Spectral	0.87	1.37		
MODIS	0.86	4.24	0.91	4.21
Landsat	0.5	4.68	0.45	4.71

The percent cover of PV, NPV, and BS calculated for the in situ and image-based method at each field site (Figure 5) shows the in situ methods varied significantly. For Fowlers Gap sites 2–4, the step-point and spectral PV, NPV, and BS were very similar, whereas at the Fowlers Gap site 1 and the Broken Hill sites, PV followed a similar pattern but NPV and BS varied significantly from one another. Overall, PV was low across all sites and especially low for the Fowlers Gap sites, with approximately 10% less PV than the Broken Hill sites. As shown in Figure 3a,b, Fowlers Gap vegetation was extremely sparse with vast areas of exposed soil, and while the Broken Hill sites were also sparsely vegetated, they still had considerably more vegetation than the Fowlers Gap sites.

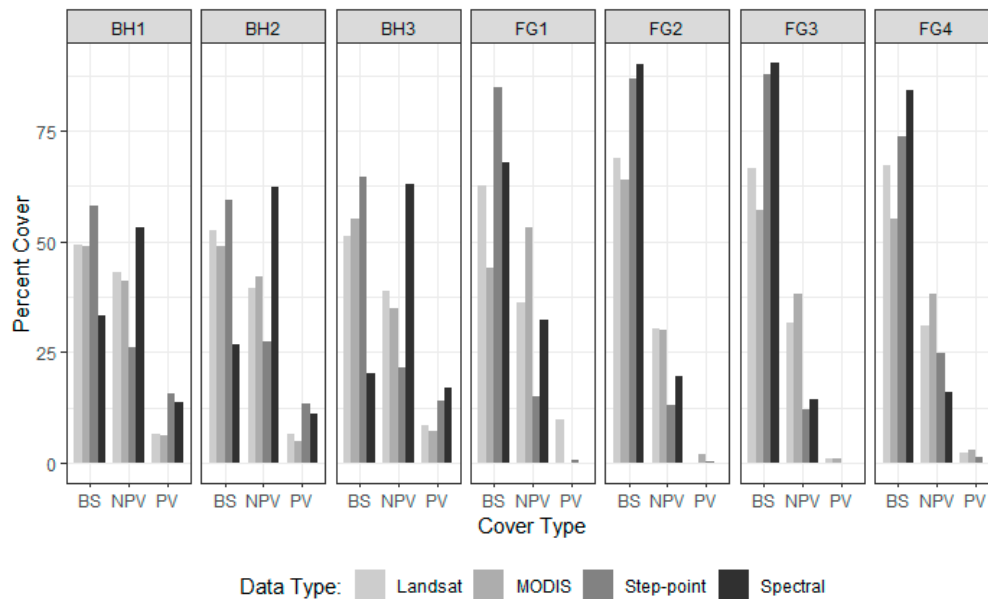


Figure 5. Summary of the fractional cover at each survey site calculated for each survey method.

4. Discussion

The motivation for this study was to test field-based hyperspectral ground cover sampling as a method of calibrating and validating image-based fractional ground cover products in Australia. By developing an alternative survey design for spectral transect sampling and comparing this method to step-point sampling at the same spatial scale, we developed an insight into the relationship between our two field methods and how they compare to current Australian image-derived fractional ground cover products.

Overall, the in situ methods were positively correlated with each other. Though neither method is truly ‘ground truth’, this strong positive linear relationship between the in situ methods suggests they provided relatively accurate estimates of ground cover at each field site. In contrast, Meyer and Okin [35] found little to no correlation between their two field methods. This is likely due to a scale mismatch in the Meyer and Okin study (the line point transects were 100 m, and the spectral transects were 500 m), whereas we avoided this mismatch by conducting both surveys over the same 500-m transects. Additionally, by avoiding a star-transect layout, our grid sample design more evenly distributed sample points across each site, ensuring that that we were not over sampling a specific area and collecting data evenly across each site.

Overall, there was relatively good correlation between both in situ methods and the image-based products. Previous validation of the MODIS and Landsat methods using in situ measurements similar to our step-point sampling reported good correlation between in situ measurements and the image-based products [24,46], but very few of these sites were located in areas with a very low percentage of vegetation. MAE was consistently low between the in situ measurements and image-based values for PV compared to BS and NPV, which showed considerably higher errors (Table 1). This pattern of errors

is also consistent with past studies, where PV has been successfully unmixed due to being spectrally unique, whereas BS and NPV are typically harder to distinguish due to their spectral similarity [15,35].

The observer and the spectral field data recorded less than 1.3% PV at the Fowlers Gap site, MODIS PV values ranged from 0% to 3%, and Landsat ranged from 0% to 9.72% PV. Considering the finer resolution of the Landsat product, we would have expected PV to be better correlated with the Landsat values rather than the MODIS values. A reason for this could be related to the image products. The Landsat FC product is based on a single image captured on one day, whereas the MODIS MCD43A4 product calculates the weighted estimate of albedo over a 16-day period. The Landsat image was captured during this 16-day composite period.

This comparison was conducted with a small number of samples located in the arid zone where we know these products tend to fail [19,24]. More extensive surveys are needed to determine if this pattern is more widespread in arid areas. It is also important to remember that we compared single MODIS pixels with an average of 400 Landsat pixels. Sampling a cluster of pixels is preferable for accuracy assessment to remove errors associated with positional accuracy [48]. This is feasible for image products with resolutions of 5, 10, or 30 m but becomes logistically taxing for clusters of MODIS pixels at 500 m. This is why the upscaling of field data is regularly used. Currently, the MODIS product is validated using upscaled in situ data initially collected over 100-m transects. Sampling the area of a single pixel in the field has limitations. We argue that overall, surveying the area of a single MODIS pixel is preferable to comparing upscaled field data to a MODIS pixel.

Arid shrublands and desert zone cover 48% of the Australian continent [49]. Having reliable long-term fractional cover data at varying scales is crucial for those managing or studying these regions, especially for areas that are inaccessible or unsafe to travel. The in situ methods used have both benefits and shortcomings. Step-point sampling has been developed over time as a simple and easily repeatable method of collecting fractional ground cover estimates. Limitations of this technique include the time-consuming collection of field observations and the potential for human subjectivity and bias to be introduced, especially when classifying PV and NPV [32]. Utilizing standardized definitions and methods [30] may reduce subjective error but cannot remove it entirely. In order to further reduce human bias, spectral transect sampling provides a solution. This method allows for continuous, quantitative hyperspectral measurements to be taken over an area, providing an objective record of ground cover without the need for observers to make categorical decisions in the field. This hyperspectral record of ground cover may also have the potential to calibrate and validate a range of other remotely sensed products and this is an area of future research. With the continued demand for high-quality ground cover products, it is critical to ensure that we are collecting high-quality calibration and validation data for the assessment of these sought-after products.

5. Conclusions

Field-based estimation of fractional ground cover is critical for ensuring the accuracy and consistency of remotely sensed ground cover maps. Currently, Australia's national standard for the collection of field estimates of ground cover uses traditional field sampling techniques, but hyperspectral reflectance sampling of ground cover has considerable potential to improve field measurements collected for calibration and validation purposes. This study trailed the use of hyperspectral reflectance sampling in the sparsely vegetated NSW arid zone. Comparison of step-point and spectral transect sampling across the same transects, at the same spatial scale, demonstrated the significant potential of the spectral transect method, both in its ability to produce results comparable to the traditional transect measures and also in the improved objectivity and relative logistic ease of the method.

Overall, we found the in situ step-point and spectral sampling techniques to be positively correlated across the three ground cover classes. Comparing the in situ data and current Australian image-derived fractional cover products showed that overall, the Landsat product was strongly related to both in situ methods for non-photosynthetic vegetation and bare soil whereas the MODIS product

was strongly correlated with both in situ methods for photosynthetic vegetation. These results are specific to our survey sites and further work is required to test their wider applicability.

While a limitation of spectral sampling is the availability and cost of the spectroradiometer itself, overall, the benefits outweigh the limitations. Spectral sampling is especially beneficial for repeat surveys or multi-temporal studies. Future efforts should be made to include spectral ground cover sampling as part of Australia's efforts to produce calibration and validation datasets for remotely sensed products and should further test this method to develop a national or global standard.

Author Contributions: Conceptualization, C.F.; methodology, C.F., K.D.C., M.M.L.; data curation, C.F.; formal analysis, C.F.; writing—original draft preparation, C.F., K.D.C. and M.M.L.; writing—review and editing, C.F., K.D.C., and M.M.L.

Funding: This research received no external funding.

Acknowledgments: I would like to thank my field assistant Hannah Auricht for giving up her time and for being great company in the field. Thank you to Keith Leggit for granting permission to work on UNSW Fowlers Gap Research Station and to Vikki Dowling for providing excellent accommodation. Lastly, thank you to the Broken Hill City Council and the Rangers at the Living Desert for permission to work on the reserve. Financial support for this research was provided by the Australian Government Research Training Program Scholarship and the University of Adelaide School of Biological Sciences.

Conflicts of Interest: The authors declare no conflict of interest.

References

1. Ma, X.; Huete, A.; Yu, Q.; Coupe, N.R.; Davies, K.; Broich, M.; Ratana, P.; Beringer, J.; Hutley, L.B.; Cleverly, J.; et al. Spatial patterns and temporal dynamics in savanna vegetation phenology across the North Australian tropical transect. *Remote Sens. Environ.* **2013**, *139*, 97–115. [[CrossRef](#)]
2. Gan, M.Y.; Deng, J.S.; Zheng, X.Y.; Hong, Y.; Wang, K. Monitoring urban greenness dynamics using multiple endmember spectral mixture analysis. *PLoS ONE* **2014**, *9*, 12. [[CrossRef](#)] [[PubMed](#)]
3. Quintano, C.; Fernández-Manso, A.; Roberts, D.A. Multiple endmember spectral mixture analysis (mesma) to map burn severity levels from Landsat images in mediterranean countries. *Remote Sens. Environ.* **2013**, *136*, 76–88. [[CrossRef](#)]
4. Mayes, M.T.; Mustard, J.F.; Melillo, J.M. Forest cover change in miombo woodlands: Modeling land cover of african dry tropical forests with linear spectral mixture analysis. *Remote Sens. Environ.* **2015**, *165*, 203–215. [[CrossRef](#)]
5. Karimi, N.; Golian, S.; Karimi, D. Monitoring deforestation in Iran, Jangal-abr forest using multi-temporal satellite images and spectral mixture analysis method. *Arab. J. Geosci.* **2016**, *9*, 1–16. [[CrossRef](#)]
6. Settle, J.; Drake, N. Linear mixing and the estimation of ground cover proportions. *Int. J. Remote Sens.* **1993**, *14*, 1159–1177. [[CrossRef](#)]
7. Smith, M.O.; Ustin, S.L.; Adams, J.B.; Gillespie, A.R. Vegetation in deserts. I. A regional measure of abundance from multispectral images. *Remote Sens. Environ.* **1990**, *31*, 1–26. [[CrossRef](#)]
8. Adams, J.B.; Smith, M.O.; Johnson, P.E. Spectral mixture modeling: A new analysis of rock and soil types at the viking lander 1 site. *J. Geophys. Res. Solid Earth* **1986**, *91*, 8098–8112. [[CrossRef](#)]
9. Roberts, D.A.; Gardner, M.; Church, R.; Ustin, S.; Scheer, G.; Green, R.O. Mapping Chaparral in the Santa Monica mountains using multiple endmember spectral mixture models. *Remote Sens. Environ.* **1998**, *65*, 267–279. [[CrossRef](#)]
10. Okin, G.S. Relative spectral mixture analysis—A multitemporal index of total vegetation cover. *Remote Sens. Environ.* **2007**, *106*, 467–479. [[CrossRef](#)]
11. Baret, F.; Weiss, M.; Lacaze, R.; Camacho, F.; Makhmara, H.; Pacholczyk, P.; Smets, B. Geov1: Lai and fapar essential climate variables and fcover global time series capitalizing over existing products. Part 1: Principles of development and production. *Remote Sens. Environ.* **2013**, *137*, 299–309. [[CrossRef](#)]
12. Camacho, F.; Cernicharo, J.; Lacaze, R.; Baret, F.; Weiss, M. Geov1: Lai, fapar essential climate variables and fcover global time series capitalizing over existing products. Part 2: Validation and intercomparison with reference products. *Remote Sens. Environ.* **2013**, *137*, 310–329. [[CrossRef](#)]

13. Awad, J.; Fisk, C.A.; Cox, J.W.; Anderson, S.J.; van Leeuwen, J. Modelling of THM formation potential and DOM removal based on drinking water catchment characteristics. *Sci. Total Environ.* **2018**, *635*, 761–768. [[CrossRef](#)] [[PubMed](#)]
14. Powell, R.L.; Roberts, D.A.; Dennison, P.E.; Hess, L.L. Sub-pixel mapping of urban land cover using multiple endmember spectral mixture analysis: Manaus, Brazil. *Remote Sens. Environ.* **2007**, *106*, 253–267. [[CrossRef](#)]
15. Mishra, N.B.; Crews, K.A.; Okin, G.S. Relating spatial patterns of fractional land cover to savanna vegetation morphology using multi-scale remote sensing in the Central Kalahari. *Int. J. Remote Sens.* **2014**, *35*, 2082–2104.
16. Guerschman, J.P.; Hill, M.J.; Renzullo, L.J.; Barrett, D.J.; Marks, A.S.; Botha, E.J. Estimating fractional cover of photosynthetic vegetation, non-photosynthetic vegetation and bare soil in the Australian tropical savanna region upscaling the EO-1 Hyperion and MODIS sensors. *Remote Sens. Environ.* **2009**, *113*, 928–945. [[CrossRef](#)]
17. Thomas, V.; Treitz, P.; Jelinski, D.; Miller, J.; Lafleur, P.; McCaughey, J.H. Image classification of a northern peatland complex using spectral and plant community data. *Remote Sens. Environ.* **2003**, *84*, 83–99. [[CrossRef](#)]
18. Artigas, F.J.; Yang, J.S. Hyperspectral remote sensing of marsh species and plant vigour gradient in the New Jersey meadowlands. *Int. J. Remote Sens.* **2005**, *26*, 5209–5220. [[CrossRef](#)]
19. Guerschman, J.P.; Oyarzabal, M.; Malthus, T.; McVicar, T.; Byrne, G.; Randall, L.; Stewart, J. *Evaluation of the MODIS-Based Vegetation Fractional Cover Product*; CSIRO: Canberra, Australia, 2012; pp. 1–28.
20. Lawley, E.F.; Lewis, M.M.; Ostendorf, B. Evaluating MODIS soil fractional cover for arid regions, using albedo from high-spatial resolution satellite imagery. *Int. J. Remote Sens.* **2014**, *35*, 2028–2046.
21. Montesano, P.; Nelson, R.; Sun, G.; Margolis, H.; Kerber, A.; Ranson, K. MODIS tree cover validation for the circumpolar taiga–tundra transition zone. *Remote Sens. Environ.* **2009**, *113*, 2130–2141. [[CrossRef](#)]
22. Morissette, J.T.; Nickeson, J.E.; Davis, P.; Wang, Y.; Tian, Y.; Woodcock, C.E.; Shabanov, N.; Hansen, M.; Cohen, W.B.; Oetter, D.R. High spatial resolution satellite observations for validation of MODIS land products: Ikonos observations acquired under the NASA scientific data purchase. *Remote Sens. Environ.* **2003**, *88*, 100–110. [[CrossRef](#)]
23. Xiao, J.; Moody, A. A comparison of methods for estimating fractional green vegetation cover within a desert-to-upland transition zone in central New Mexico, USA. *Remote Sens. Environ.* **2005**, *98*, 237–250. [[CrossRef](#)]
24. Scarth, P.; Röder, A.S.M.; Denham, R. Tracking Grazing Pressure and Climate Interaction—The Role of Landsat Fractional Cover in Time Series Analysis. In Proceedings of the 15th Australasian Remote Sensing and Photogrammetry Conference, Alice Springs, Australia, 13–17 September 2010.
25. Asner, G.P.; Heidebrecht, K.B. Spectral unmixing of vegetation, soil and dry carbon cover in arid regions: Comparing multispectral and hyperspectral observations. *Int. J. Remote Sens.* **2002**, *23*, 3939–3958. [[CrossRef](#)]
26. Lewis, M.M. Numeric classification as an aid to spectral mapping of vegetation communities. *Plant Ecol.* **1998**, *136*, 133. [[CrossRef](#)]
27. Winkworth, R.; Perry, R.; Rossetti, C. A comparison of methods of estimating plant cover in an arid grassland community. *J. Range Manag.* **1962**, 194–196. [[CrossRef](#)]
28. Graham, F.G. An enhanced wheel-point method for assessing cover, structure and heterogeneity in plant communities. *J. Range Manag.* **1989**, *42*, 79–81.
29. Evans, R.A.; Love, R.M. The step-point method of sampling—a practical tool in range research. *Rangeland Ecol. Manag. J. Range Manag. Arch.* **1957**, *10*, 208–212. [[CrossRef](#)]
30. Muir, J.; Schmidt, M.; Tindall, D.; Trevithick, R.; Scarth, P.; Stewart, J. Field measurement of fractional ground cover: A technical handbook supporting ground cover monitoring for Australia. *ABARES Canberra ACT* **2011**, 1–58. Available online: https://daff.ent.sirsidyntix.net.au/client/en_AU/search/asset/1027474/0 (accessed on 12 July 2017).
31. Trevithick, R.; Muir, J.; Denham, R. The effect of observer experience levels on the variability of fractional ground cover reference data. In Proceedings of the XXII Congress of the International Photogrammetry and Remote Sensing Society, Melbourne, Australia, 25 August–1 September 2012.
32. Fisk, C.; Clarke, K.D.; Delean, S.; Lewis, M.M. Distinguishing photosynthetic and non-photosynthetic vegetation: How do traditional observations and spectral classification compare? *Remote Sens.* **2019**, *11*, 2589. [[CrossRef](#)]

33. Li, F.; Jupp, D.L.B.; Reddy, S.; Lyburner, L.; Mueller, N.; Tan, P.; Islam, A. An evaluation of the use of atmospheric and BRDF correction to standardize Landsat data. *IEEE J. Sel. Top. Appl. Earth Observ. Remote Sens.* **2010**, *3*, 257–270. [CrossRef]
34. Liang, S.; Fang, H.; Chen, M.; Shuey, C.J.; Walthall, C.; Daughtry, C.; Morisette, J.; Schaaf, C.; Strahler, A. Validating MODIS land surface reflectance and albedo products: Methods and preliminary results. *Remote Sens. Environ.* **2002**, *83*, 149–162. [CrossRef]
35. Meyer, T.; Okin, G.S. Evaluation of spectral unmixing techniques using MODIS in a structurally complex savanna environment for retrieval of green vegetation, nonphotosynthetic vegetation, and soil fractional cover. *Remote Sens. Environ.* **2015**, *161*, 122–130. [CrossRef]
36. Lewis, M. Discrimination of arid vegetation composition with high resolution casi imagery. *Rangeland J.* **2000**, *22*, 141. [CrossRef]
37. White, A.; Sparrow, B.; Leitch, E.; Foulkes, J.; Flitton, R.; Lowe, A.J.; Caddy-Retalic, S. *Ausplots Rangelands Survey Protocols Manual*; University of Adelaide Press: Adelaide, Australia, 2012; Available online: <https://www.tern.org.au/AusPlots-Rangelands-Survey-Protocols-Manual-pg23944.html> (accessed on 24 August 2016).
38. Stern, H.; De Hoedt, G.; Ernst, J. Objective classification of Australian climates. *Austr. Meteorol. Mag.* **2000**, *49*, 87–96.
39. Bureau of Meteorology. Climate Statistics for Australian Locations—Summary Statistics Fowlers Gap AWS. 2019. Available online: http://www.bom.gov.au/climate/averages/tables/cw_046128.shtml (accessed on 12 July 2019).
40. Mabbutt, J.A.; Burrell, J.P.; Corbett, J.R.; Sullivan, M.E. *Land Systems of Fowlers Gap Station*; University of New South Wales: Sydney, Australia, 1973; pp. 25–43.
41. Bureau of Meteorology. Climate Statistics for Australian Locations—Summary Statistics Broken Hill Airport AWS. Available online: http://www.bom.gov.au/climate/averages/tables/cw_047048.shtml (accessed on 12 July 2019).
42. Benson, J. *Setting the Scene: The Native Vegetation of New South Wales*; Background Paper; Native Vegetation Advisory Council: Sydney, Australia, 1999.
43. Analytical Spectral Devices. In *Fieldspec 3 User Manual*; ASD Inc.: Boulder, Colorado, 2008.
44. Gruninger, J.; Ratkowski, A.J.; Hoke, M.L. *The Sequential Maximum Angle Convex Cone (Smacc) Endmember Model*; Spectral Sciences Inc.: Burlington, MA, USA, 2004.
45. Adams, J.B.; Smith, M.O.; Gillespie, A.R. Imaging spectroscopy: Interpretation based on spectral mixture analysis. In *Remote Geochemical Analysis: Elemental and Mineralogical Composition*; Cambridge University Press: New York, NY, USA, 1993; pp. 145–166.
46. Guerschman, J.P.; Hill, M.J. Calibration and validation of the Australian fractional cover product for MODIS collection 6. *Remote Sens. Lett.* **2018**, *9*, 696–705. [CrossRef]
47. Geoscience Australia. Fractional Cover (fc25) Product Description. 2015. Available online: https://d28rz98at9flks.cloudfront.net/79676/Fractional_Cover_FC25_v1_5.PDF (accessed on 12 March 2019).
48. Congalton, R.G.; Green, K. *Assessing the Accuracy of Remotely Sensed Data: Principles and Practices*; CRC Press: Boca Raton, FL, USA, 2008.
49. Department of the Environment. *Conservation Management Zones of Australia*; Australian Government: Canberra, Australia, 2015.

